SUBSTRUCTURE MODEL FOR CONCRETE BEHAVIOR SIMULATION UNDER CYCLIC MULTIAXIAL LOADING

A.A. Khosroshahi and S.A. Sadrnejad*

Department of Civil Engineering, K.N. Toosi University of Technology
P.O. Box 15878-4416, Tehran, Iran
a.khosroshahi@sazeh.co.ir - sadrnejad@kntu.ac.ir

*Corresponding Author

(Received: August 17, 2006 – Accepted in Revised Form: May 9, 2008)

Abstract This paper proposes a framework for the constitutive model based on the semi-micromechanical aspects of plasticity, including damage progress for simulating behavior of concrete under multiaxial loading. This model is aimed to be used in plastic and fracture analysis of both regular and reinforced concrete structures, for the framework of sample plane crack approach. This model uses multilaminated framework with sub-loading surface to provide isotropic and kinematics hardening/softening in the ascending/descending branches of loading. In multilaminated framework a relation between stress/strain and yield function on planes of various orientation is defined and stress/strain path history for each plane is kept for a sequence of future analysis. Four basic stress states including compression-shear with increase/decrease in the compression/shear ratio,tension-shear and pure compression are defined and the constitutive law for each plane is derived from the most influenced combination of stress states. With using sub-loading aspect of the surface, the kinematics and isotropic hardening are applied to the model to make it capable of simulating the behavior under any stress path, such as cyclic loading in the ascending/descending branch of loading. Based on the experimental results of the literature, the model parameters are calibrated. The model results under monotonic loading and also different states of cyclic loadings such as uniaxial compression, tension, alternate compression tension, shear and triaxial compression are compared with experimental results that shows the capability of the model.

Keywords Concrete, Multilaminate, Microplane, Elastoplastic, FEM, Substructure, Fracture

چکیده این مقاله به ارائه چهار چوبی برای الگوی ساختاری براساس مفهوم شبهه ریز خمیری شامل پیشرفت آسیب دیدگی برای شبیه سازی رفتار بتن تحت بارگذاری چند محوری می‌پردازد. این الگو به هدف استفاده در تحلیل های خمیری شکست بتن و سازه های بتنی مسلح در چهارچوب تقریب ترک روی صفحات نمونه است و براساس چهارچوب چند صفحه ای با استفاده از سطح زیر بارگذاری و سخت شدگی/نرم شدگی همسان و حرکتی در شاخه های سربالائی/سرپائینی بارگذاری می باشد. در چهارچوب چند صفحه ای ارتباط بین تنش/کرنش و تابع سیلان روی صفحات با جهات مختلف تعریف شده و مسیرهای تاریخچه تنش/کرنش برای هر صفحه برای مراحل بعدی تحلیل نگه داشته می‌شود. چهار حالت اساسی تنش شامل فشار برش با افزایش/کاهش در نسبت فشار/برش، کشش – برش و فشار خالص تعریف شده و قانون ساختاری برای هر صفحه برای بیشترین تاثیر ترکیب حالات تنش بدست آورده می‌شود. با استفاده از مفهوم سطح زیر بارگذاری سخت شدگی همسان و حرکتی در الگو اعمال گردیده و الگو قادر به شبیه سازی رفتار تحت هر مسیر تنش از جمله بارهای چرخه ای در شاخه های سربالائی/سرپائینی بارگذاری می‌باشد. براساس نتایج آزمایشگاهی الگو فراسنجی گردید و نتایج الگو تحت بارگذاری تک گامه و همچنین حالات مختلف بار چرخه ای مانند فشار تک محوری، کشش، فشار–کشش متناوب، برش و فشار سه محوری با نتایج آزمایشگاهی مقایسه گردید که نشان دهنده قابلیت الگو است.

1. INTRODUCTION

A simulation of concrete behavior and fractured mechanism of concrete, under different states of multiaxial stresses, load paths, also the prediction of aspects such as unloading/reloading and cyclic

loading is very significant. Several models are used in the recent years based on the stress/strain invariants, the classical approach to constitutive modeling of concrete based on direct use of stress/strain tensor, and their invariants were used in the first decade of computer programming, and there hasn't been any more accurate modeling of concrete since. However the models based on the concrete sub-structures, such as microplane and multilaminated could improve concrete modeling specially where the concrete is non-isotropic or there is fabric property or even a crack in the concrete. The proposed model is able to predict the behavior of concrete under any arbitrary stress/strain path and final failure mechanism.

1.1. Multilaminate Concept The concept of multilaminate is based on the numerical approximation of integration, and the distribution of a certain physical property such as strain distributed over the surface of a media. This approach can numerically be achieved by summing up the multiplication of the property values by the specified weighted coefficients for predefined points and considering as an approximate representative value over the media. Based on this framework the behavior of a three dimensional media is averaged and approximated into the appropriate summation of slipping behavior of sampling planes passing through points. Consequently, this slip feature could be representative of the real variations of strain which are taken place through the boundaries of artificial structural units. Therefore, the accuracy of the solutions is highly related to the employed constitutive relation for the frictional slip/ opening/closing gaps of a sampling point.

1.2. History of Multilaminate Framework The concept of multilaminate approach was first proposed by Taylor in 1938 [1]. Later a theory of plasticity based on the concept of slip theory was developed by Batdorf, et al [2] and Budiansky for metals. This theory was based on the assumption that, slip in any particular orientation in the material, will develop to a plastic shear strain which depends only on the history of the corresponding component of shear stresses/strains.

Multilaminates model for rocks was developed by Zienkiewicz, et al [3], Also Pande, et al [4] developed elasto/viscoplastic model for clays.

Bazant, et al [5] developed a model called microplane model for fracture analysis of concrete. This model was proposed to describe inelastic decline of stress at increasing strain which results to from progressive development of fracture and was based on the strain control parameters and summation of stress increments on each plane with using equivalent virtual energy to obtain macro-stress.

Sadrnejad, et al [6,7] developed a multilaminate model for granular materials and in particular sands.

2. MODEL EXPLANATION

The proposed model is originally based on the multi-laminated framework for elastoplastic behavior of intact concrete, sub-structural boundaries, considering hardening/softening rule and elastic behavior of sub-structural units. It consists of the following basis:

- Constitutive equations
- Yield function and potential surface
- Hardening/Softening rule
- Flow rule and consistency condition

2.1. General Constitutive Equation From classical theory strain can be decomposed to elastic and plastic components as follow:

$$d\varepsilon = d\varepsilon^{e} + d\varepsilon^{P}$$

$$d\varepsilon^{e} = C^{e} d\sigma$$

$$d\varepsilon^{P} = C^{p} d\sigma$$

C^{e} is the elastic part of compliance matrix and C^{P} is the plastic compliance matrix. C^{e} is constant for different planes and is computed from elasticity theory.

The term $d\varepsilon^{P}$ can be calculated from weighted summation of $d\varepsilon_{i}^{p}$ of active planes, if a sphere with

n planes is considered as shown in Figure 1:

$$d\varepsilon^{P} = 8\pi \sum_{i=1}^{n} W_i [L_\varepsilon]^T . d\varepsilon_i^p$$

With considering $d\varepsilon_i^p = \bar{C}_i^p d\sigma_i$

$$d\varepsilon^{P} = 8\pi \sum_{i=1}^{n} W_i [L_\varepsilon]^T . \bar{C}_i^p . [L_\sigma] . d\sigma$$

$$C_i^p = [L_\varepsilon]^T . \bar{C}_i^p . [L_\sigma]$$

$$C^{P} = 8\pi \sum_{i=1}^{n} W_i . C_i^p .$$

Where L_ε and L_σ are transformation matrices for strain and stresses, respectively n is number of planes. $\bar{C}_i^p$ is 3 x 3 compliance matrix for plane i in the local coordinates and C_i^p is 6 x 6 compliance matrix in the global coordinate.

C^p is composed from weighted summation of C_i^p corresponding to any of the active planes, It should be noted that C_i^p for elastic planes (Non-active planes) is equal Zero, Analysis shows that using 13 planes satisfy accuracy for most engineering problems. These planes are shown in the Figure 2

A modified Sub-loading yield surface is used in the models [8,9], for elasto-plastic behavior of planes as shown in Figure 3 sub-loading surface,which always passes through the current stress point and keeps a similar shape to the yield surface, therefore renamed as the normal-yield surface, and an orientation of similarity to the normal-yield surface. The subloading surface does not only translate but also expands/contracts with the plastic deformation.

The similarity-center S moves with a plastic deformation. Although it was fixed in the origin of stress space in the initial subloading surface model, using this concept the model has strong capability to predict isotropic and kinematics hardening behavior for loading, unloading and reloading.

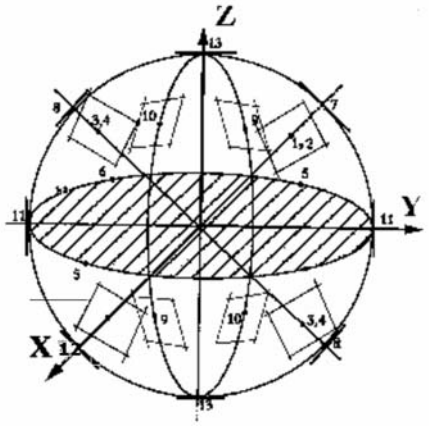

Figure 1. Multilaminate framework aspect and planes orientations.

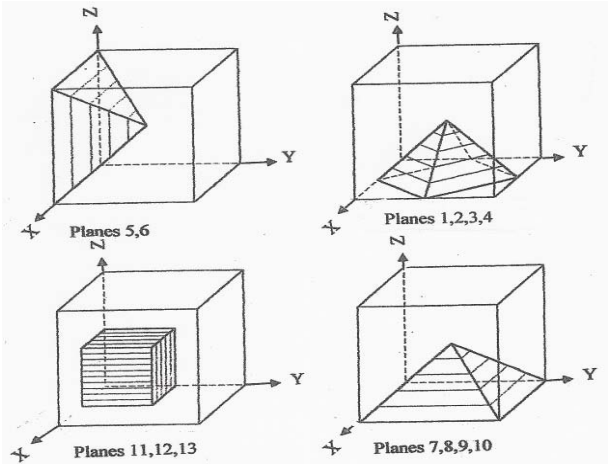

Figure 2. Multilaminate planes orientations.

2.2. Stress State on Planes The effects of any stress/strain path over a simple typical dx,dy,dz cube element on an arbitrary sampling plane can lead to four stress/strain paths. All stress states in the material can be divided to four categories on a typical plane which are as follows:

- Compression-Shear with Increasing in the Compression
- Compression-Shear with Decreasing in the Compression
- Tension-Shear
- Pure Compression

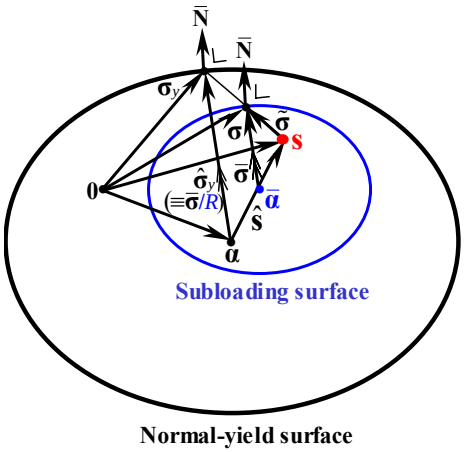

Figure 3. Normal-yield and Subloading surfaces.

In this framework, any form of yield criterion including crack effects may be considered for different sampling plane to any local behavior aspect, and with the summation of all planes behavior we approach the media behavior.

In most cases of element stress/strain paths the compression or tension, accompanied shear is the governing case, but for generality of the model, pure compression is considered in the model. In this way any complex form of stress/strain path is analysed into the stated four, on the planes cases and lead to proper planar behavior.

The yielding criteria proposed for the identified cases are introduced as follow:

2.2.1. Compression-shear When a plane is subjected to compression and shear in the loading path, two load pattern may exist:

- ❖ Increasing or constant shear/compression rate with increase in the compression stress, sample of this load path is Triaxial compression test with the constant lateral pressure and increasing axial compression stress. The uniaxial compression is a special case that shear/compression ratio is constant.
- ❖ Increasing shear/compression rate with decreasing compression stress. Sample with this load pattern is a triaxial test, when the lateral compression is decreased but axial compression is remained.

The behavior of concrete under the above load paths is not completely similar thus two separate functions are used in the equations.

2.2.1.1. Increasing Shear/Compression Rate With Increase in the Compression Stress In this models' hyperbolic yield function for compressive and shear stresses is considered as follows:

$$f(\hat{\sigma}) = \tau - C_H(\sigma_n + C_3\sigma_n^2) \le F(H)$$

$$\tau = \sqrt{\hat{\sigma}_y^2 + \hat{\sigma}_z^2}$$

$$\sigma_n = \sigma_x$$

C_3 = Material constant

F(H) = Hardening/Softening Function

$$F(H) = v_2(1 + C_1(H_i / H_m) + v_4, H_i \le H_m$$

$$F(H) = v_2(1 + C_1(H_i / H_m) + v_2.C_2(H_i / H_m - 1) + v_4, H_i > H_m$$

$$H_i = \varepsilon_{si} = \sqrt{\varepsilon_{xi}^{p2} + \varepsilon_{yi}^{p2} + \varepsilon_{zi}^{p2}}$$ Plastic strain

$H_m = v_1$ = Model variable

C_1, C_2 Material constants

v_2 Material Strength variable

C_{Hi} Hystersis softening parameter

$$C_{Hi} = v_3.e^{A_i(H_i - H_{0i})} - (SIGN.v_3 - C_{H0i})e^{A_i(H_i - H_{0i})} - C_{11}(1 - SIGN)(C_4.v_3 - C_{h0i})e^{A_i(H_I - H_{0i})}$$

SIGN = 1 for loading/reloading; SIGN = -1 for unloading; at the end of previous cycle $C_{H0i} = C_{Hi}$ value, it may be $C_{H0i} = v_3.C_4$ for first loading.

The term H_{0i} is value of H_i at the end of previous cycle in the first loading (virgin material) and it is zero. If the previous load path is pure

compression $H_{0i} = C_{14}\varepsilon_{v\max}$.

The term A_i is cyclic parameter. At the first loading, it is C_{12}. Then it becomes:

$$A_i = C_{12} + C_{13}.H_{0i}$$

at the end of previous cycle.

All active planes in the state of loading such as uniaxial compression, Biaxial Compression, Triaxial Compression and also some planes in the Biaxial Compression-Tension test can be categorized in the compression-Shear state. Also it should be noted that some planes, for example plane normal to load in uniaxial compression test is in pure compression, but this plane remains elastic in the test.

2.2.1.2. Increasing Shear/Compression Rate With Decrease in Compression Stress In the model yield function is similar to increasing compression stress except the C_3 is revised to C_5 as follows:

$$f(\hat{\sigma}) = \tau - C_H(\sigma_n + C_5\sigma_n^2) \le F(H)$$

2.2.2.Tension-shear In this model mohr-Coloumb linear yield function between tension stress and shear stress is used:

$$f(\hat{\sigma}) = \tau - C_H\sigma_n \le F_T(H)$$

$$\tau = \sqrt{\hat{\sigma}_y^2 + \hat{\sigma}_z^2}$$

$$\sigma_n = \sigma_x$$

$$F_T(H) = (v_2 + v_4)e^{C_8H_i}$$

Hardening is considered in the C_H as frictional hardening/softening including degrading in the cyclic hystersis behavior also $F_T(H_i)$represents cohesional hardening/softening and when the crack opens the cohesional strength of material is considered as zero but the frictional strength is remained.

2.2.3. Pure compression state For pure compression exponential function is used as follows:

$$\sigma_n = E_c v_5 \mathrm{Exp}(-C_9\varepsilon_v) - E_c v_5$$

$$\hat{f}(\sigma) = -\sigma_n + v_5E_c\mathrm{Exp}(-C_9\varepsilon_v) - E_cv_5$$

$$\varepsilon_v = (\varepsilon_n + \varepsilon_y + \varepsilon_z)/3$$

$\varepsilon_{v\max} = \mathrm{Max}\varepsilon_v$ at end of loading

C_9 = Material constants

v_5 = Material variable

Figure 4 Shows this function typically

2.3. Stresses on Planes For plane i three normal vectors is defined and stress is computed as follow:

σ_i = stress on plane i

$\vec{n}_i$ = normal cosine of plane i

$\vec{m}_i$ = arbitrary vector on plane i

$\vec{l}_i$ = vector on plane i perpendicular $\vec{m}_i$

Vector summary are as follow

2.4. Kinematic Hardening Kinematic hardening is defined as below:

$$\hat{\sigma}_i = \sigma_i - \alpha_i$$

$\hat{\alpha}_i$ = Kinematics hardening vector

$$\hat{\alpha}_i = b_i\frac{\sigma_i}{\|\sigma_i\|}$$

$$b_i = C_6H_i^{c7}$$

C_6, C_7, material constants

3. COMPUTATION PROCEDURE

The sequences of computation are as follows:

- First the stress components on each plane is calculated, then the kinematic hardening vector is calculated based on the value of the plastic strain

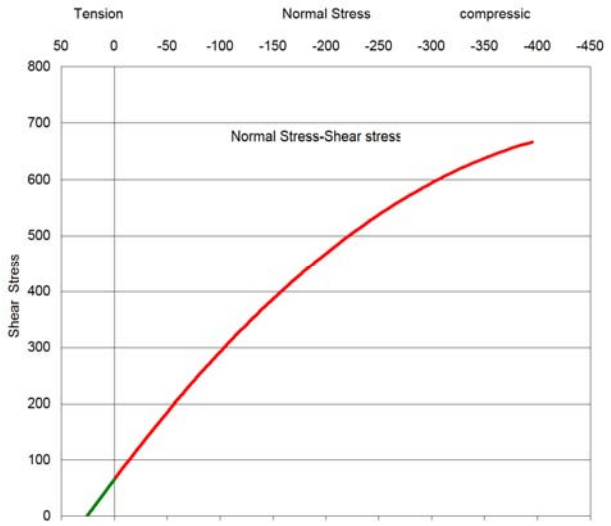

(a)

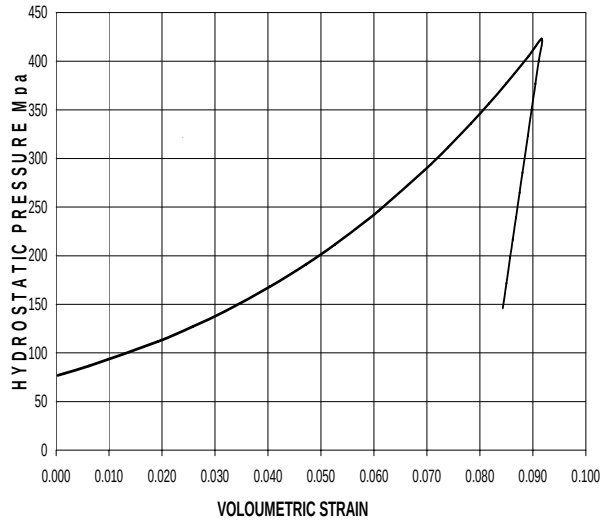

(b)

Figure 4. Typical yield function (a) Compression/tension shear (b) Pure compression.

Hi calculated from previous step. Based on the stress state of plane, the yield function is calculated. For guaranty to move in or at the surface of yield function a penalty function of U is defined as:

$$R_i = \frac{f_i(\hat{\sigma}_i)}{F_i(H_i)} \le 1.0$$

$$U_i = -u_i \ln R_i$$

$u_i = V_6$ for shear compression state

$u_i = V_7$ for shear tension state

U is the function that relates R increment to plastic strain increment and it guarantees that R_i is to be less than unit, It should be noted that in the numerical calculation R may be greater than one for 1-2 steps but the penalty function of U adjust it to unit even though the load step is large.

$$\dot{R}_i = U_i \| d\varepsilon_i^p \|$$

$$\begin{aligned} u &= \infty \quad \text{for} \quad R = 0 \\ u &> 0 \qquad\quad R < 1 \\ u &= 0 \qquad\quad R = 1 \\ u &< 0 \qquad\quad R > 1 \end{aligned}$$

Similarity center S is the center of subloading in the space of stress

$$S_i^{k+1} = S_i^k + \dot{S}_i$$

$$\dot{S} = C_{10} \| d\varepsilon^p \| \frac{\tilde{\sigma}_i}{R_i} + \dot{\alpha} + \frac{1}{F}\begin{Bmatrix} 0 \\ F\hat{S} \end{Bmatrix}$$

C_{10} = material Constant

$$\tilde{\sigma}_i = \sigma_i - S_i$$

$$\hat{S} = S_i - \alpha_i$$

$$d\varepsilon^P = \lambda \overline{N}_{NA} \quad \text{Non Associate flow Rule}$$

$$\overline{N} = \frac{\partial f(\overline{\sigma})}{\partial \sigma} / \| \frac{\partial f(\overline{\sigma})}{\partial \sigma} \| \qquad \| \overline{N} \| = 1$$

$$\overline{N}'_{NA}(1) = \frac{\partial f(\overline{\sigma})}{\partial \sigma}.C_{15} \,,$$

$$\overline{N}'_{NA}(2) = \frac{\partial f(\overline{\sigma})}{\partial \sigma} \,, \quad \overline{N}'_{NA}(3) = \frac{\partial f(\overline{\sigma})}{\partial \sigma}$$

$$\overline{N}_{NA} = \overline{N}'_{NA} / \| \overline{N}'_{NA} \|$$

C_{15} = Material Constant

$$d\varepsilon^P = \frac{tr(\overline{N}\dot{\sigma})}{\overline{M}_P}\overline{N}_{NA}$$

$$\overline{M}^P = tr\left[\overline{N}\left[\overline{a} + \left[\frac{F'}{F}h + \frac{U}{R}\right]\overline{\sigma}\right]\right]$$

$$h = \frac{\dot{H}}{\lambda}, \quad a = \frac{\dot{\alpha}}{\lambda}$$

$$\overline{a} = \frac{\dot{\alpha}}{\lambda} = (1-R)Z - U\hat{S} + Ra$$

$$Z = \frac{\dot{S}}{\lambda} = C\frac{\tilde{\sigma}}{R} + a + \frac{1}{F}F'h\hat{S}$$

$$C_i^p = \frac{tr(\overline{N}_i\dot{\sigma}_i)}{\overline{M}_i^p}N_{NA_i}$$

Then the C^p can be calculated with weighted summation of all planes.

$$C^p = 8\pi\sum_{i=1}^{13} w_i C_i^p$$

4. CALIBRATION

The parameters of models are divided into two groups, fixed parameters, that are the same for all normal concrete and need not to be calibrated for different concrete, They are parameters C_1, C_2, C_{15} and variable parameters that should be adjusted for each type of concrete such as V_1, V_2, …, V_7.

The model has been calibrated for experimental data in three stages, in the first stage the material strength under different classical load paths, such as biaxial stresses, uniaxial compression and tension, triaxial compression and shear-compression interaction is evaluated, and the parameters of most materials are defined, in the second stage the material response and strain are evaluated for many load paths such as uniaxial compression, uniaxial tension,biaxial compression, biaxial compression-tension,triaxial compression with an increase in axial compression or decrease in lateral pressure, and also concrete behavior under pure compression. In the last stage the model is evaluated for unloading, reloading and cyclic loading.

For calibration of variable parameters(V_1 to V_7) that have more effects on the model behavior, specified concrete stress-strain data for uniaxial compression, uniaxial tension and also a data for biaxial or triaxial compression strength are necessary for calibration of shear-compression and shear-tension states, and test data for pure compression should be used for calibration of model if pure compression is important. The variable parameters ranges are are shown in Table 3 (SI units).

The effect of each variable parameter on the model behavior are investigated and are as follow:

V_1	Shifts peak stress, increase strain of peak stress point
V_2	Increase concrete strength, specially shear and tensile strength
V_3	Changes stiffness and also compression strength
V_4	Controls on the pure shear strength and tensile strength
V_5	Increase material strength in pure compression
V_6	Controls material stiffness in the compression state
V_7	Controls material stiffness in the tension state

Fixed parameters (C_1 to C_{15}) has not changed in different concrete and the values set can be used for normal concrete with compressive strength between 20 MPa to 60 MPa but for high strength concrete or special concrete such as fiber reinforced concrete, these values should be adjusted, It should be noted that when more accuracy is necessary some of the fixed parameter is recommended to be adjusted, for example C_3 is very important for high confinement or C_{13} is very important for cyclic stress behavior. The typical values of fixed parameters for normal concrete are shown in Table 3.

The effect of each fixed parameter on the model

TABLE 1. Planes normal Vectors and Weights.

Plane	$\vec{n}$	$\vec{m}$	$\vec{l}$	Weight
1	$\frac{1}{\sqrt{3}}, \frac{1}{\sqrt{3}}, \frac{1}{\sqrt{3}}$	$\sqrt{\frac{1}{2}}, -\sqrt{\frac{1}{2}}, 0$	$-\sqrt{\frac{1}{6}}, -\sqrt{\frac{1}{6}}, 2\sqrt{\frac{1}{6}}$	27/840
2	$\frac{1}{\sqrt{3}}, -\frac{1}{\sqrt{3}}, \frac{1}{\sqrt{3}}$	$\sqrt{\frac{1}{2}}, \sqrt{\frac{1}{2}}, 0$	$\sqrt{\frac{1}{6}}, -\sqrt{\frac{1}{6}}, -2\sqrt{\frac{1}{6}}$	27/840
3	$-\frac{1}{\sqrt{3}}, \frac{1}{\sqrt{3}}, \frac{1}{\sqrt{3}}$	$\sqrt{\frac{1}{2}}, \sqrt{\frac{1}{2}}, 0$	$+\sqrt{\frac{1}{6}}, -\sqrt{\frac{1}{6}}, +2\sqrt{\frac{1}{6}}$	27/840
4	$-\sqrt{\frac{1}{3}}, -\sqrt{\frac{1}{3}}, \sqrt{\frac{1}{3}}$	$\sqrt{\frac{1}{2}}, -\sqrt{\frac{1}{2}}, 0$	$-\sqrt{\frac{1}{6}}, -\sqrt{\frac{1}{6}}, -2\sqrt{\frac{1}{6}}$	27/840
5	$+\sqrt{\frac{1}{2}}, \sqrt{\frac{1}{2}}, 0$	$\sqrt{\frac{1}{2}}, -\sqrt{\frac{1}{2}}, 0$	0, 0, 1	32/840
6	$-\sqrt{\frac{1}{2}}, \sqrt{\frac{1}{2}}, 0$	$\sqrt{\frac{1}{2}}, \sqrt{\frac{1}{2}}, 0$	0, 0, 1	32/840
7	$+\sqrt{\frac{1}{2}}, 0, \sqrt{\frac{1}{2}}$	$\sqrt{\frac{1}{2}}, 0, -\sqrt{\frac{1}{2}}$	0, 1, 0	32/840
8	$-\sqrt{\frac{1}{2}}, 0, \sqrt{\frac{1}{2}}$	$\sqrt{\frac{1}{2}}, 0, \sqrt{\frac{1}{2}}$	0, 1, 0	32/840
9	$0, -\sqrt{\frac{1}{2}}, \sqrt{\frac{1}{2}}$	$0, \sqrt{\frac{1}{2}}, \sqrt{\frac{1}{2}}$	1, 0, 0	32/840
10	$0, \sqrt{\frac{1}{2}}, \sqrt{\frac{1}{2}}$	$0, -\sqrt{\frac{1}{2}}, -\sqrt{\frac{1}{2}}$	1, 0, 0	32/840
11	1 , 0 , 0	0, 1, 0	0, 0, 1	40/840
12	0 , 1, 0	1, 0, 0	0, 0, 1	40/840
13	0 , 0 , 1	0, 0, 1	1, 0, 0	40/840

behavior are investigated and are as follow:

C_1,C_2	Shift post peak and effect on the residual stress
C_3	Controls strength on high pressure region specially (increasing compression)
C_4	Controls stiffness degrading
C_5	Controls strength on high pressure region specially (Decreasing compression)
C_6,C_7	Affect on the kinematic hardening
C_8	Affect on the hardening/softening in the tension state
C_9	Increase the plastic limit in pure compression
C_{10}	Control hystersis behavior and residual stress
C_{11}	Affect on the back stress in the hystersis,
C_{12} and C_{13}	Affect on the hystersis behavior
C_{14}	Relates the pure compression damage to other states of stress
C_{15}	Affect on the volumetric strain

TABLE 2. Variable Parameters Ranges.

Variable Parameter	Minimum Value	Maximum Value	Recommended Value(f'c = 40MPa)
V_1	0.005	0.05	0.01
V_2	0.2E7	0.5E7	0.3E7
V_3	0.55	0.7	0.63
V_4	0.05E7	0.2E7	0.1E7
V_5	-.002	-.005	-.003
V_6	3,000	8,000	5,000
V_7	100,000	150,000	120,000

TABLE 3. Constant Parameters.

Constant Parameter	Recommended Value (Normal Concrete)
C_1	-0.01
C_2	-0.001
C_3	3.E-9
C_4	1.8
C_5	1.5E-9
C_6	1.6E6
C_7	0.4
C_8	5000
C_9	250.
C_{10}	300
C_{11}	200
C_{12}	-55.
C_{13}	-5000.
C_{14}	0.11
C_{15}	0.20

It should be noted that if only compression-shear state is important, the strength of concrete can be adjusted with defining V_2 and V_3 and for adjusting Stiffness the variable V_6 should be adjusted, Thus for compression shear state that is most important and practical case only four variable of V_1, V_2, V_3 and V_6 are necessary, For tension and tension shear cases variable V_3, V_4 and V_7 should be adjusted too. V_5 is only significant for pure compression and high confinement pressure cases.

5. MODEL EVALUATION

As illustrated above the model has been evaluated

with experimental data from literature for its calibration and evaluations in monotonic and cyclic loading

5.1. Monotonic Loading The model is checked for different state of monotonic loadings with experimental results in the literature such as compression-shear, uniaxial compression,uniaxial tension,Biaxial compression, biaxial compression tension and triaxial compression.

Figure 5 shows the comparison of shear compression force interaction of model prediction, experimented by Bresler, et al [10] and also Goode, et al [11] that shows the strength of the model is close to experimental result.

Figure 6 shows the biaxial stress enveloped by

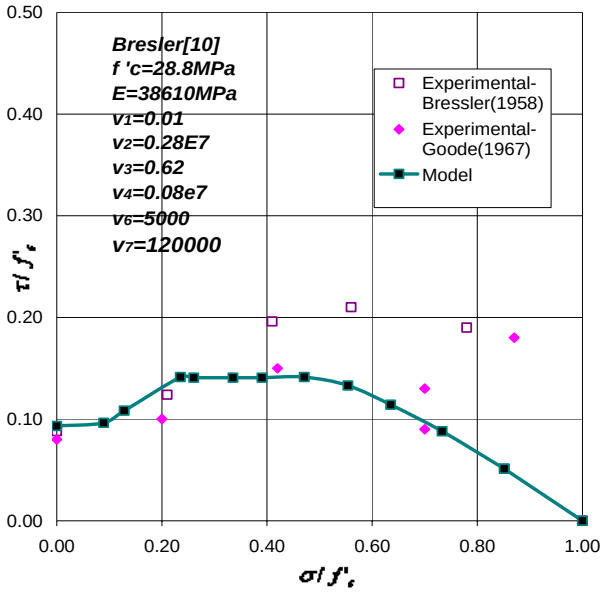

Figure 5. Comparison of model for shear-compression experimental data Bresler [10] and Goode [11].

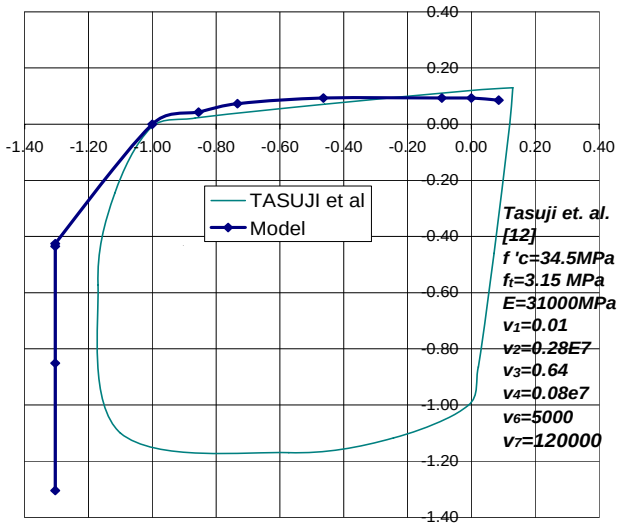

Figure 6. Comparison of model for biaxial stress experimental data, Tasuji [12].

Tasuji, et al [12] with model prediction, The model has good fitting in compression-tension and also tension-tension region but in the compression-compression region it is little more than the experimental result.

Figure 7 shows the result of uniaxial compression test (Van Mier [13]) as predicted by model that shows very good fitting of the whole response, also the volumetric strain results of the model is compared with experimental results that is quite fitted.

Figure 8 shows the comparison of uniaxial tension tests performed by Pettersson, et al [14],the model result is close to experimental data and has good fitting.

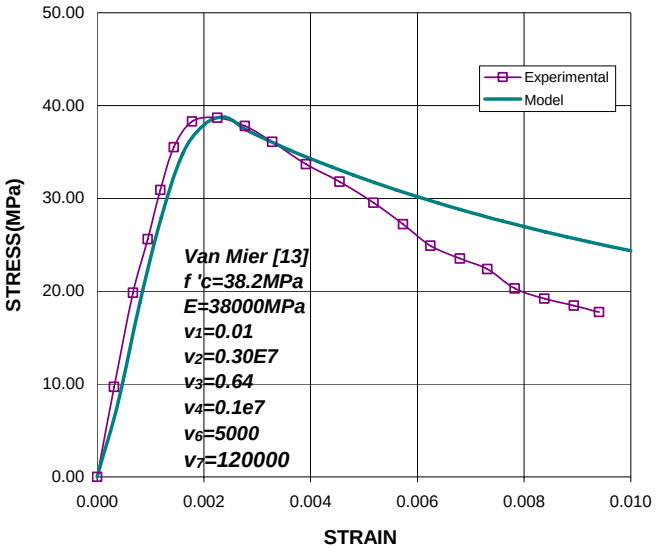

(a)

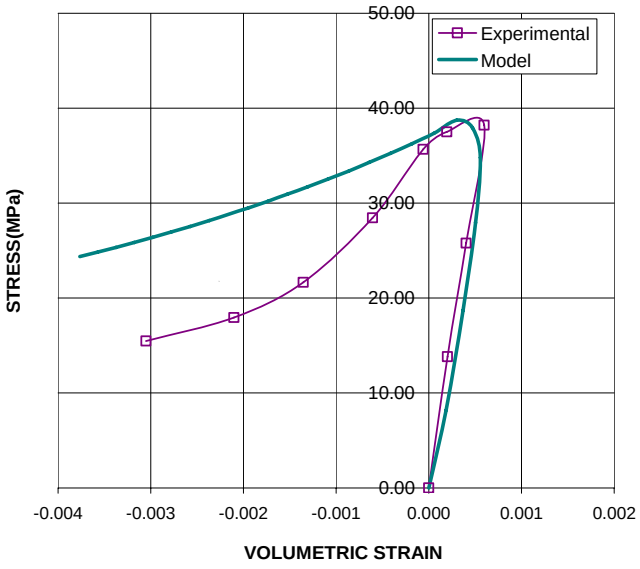

(b)

Figure 7. Comparison of model for uniaxial compression experimental data, Van mier [13] (a) Stress-strain curve (b) Volumetric strain versus stress.

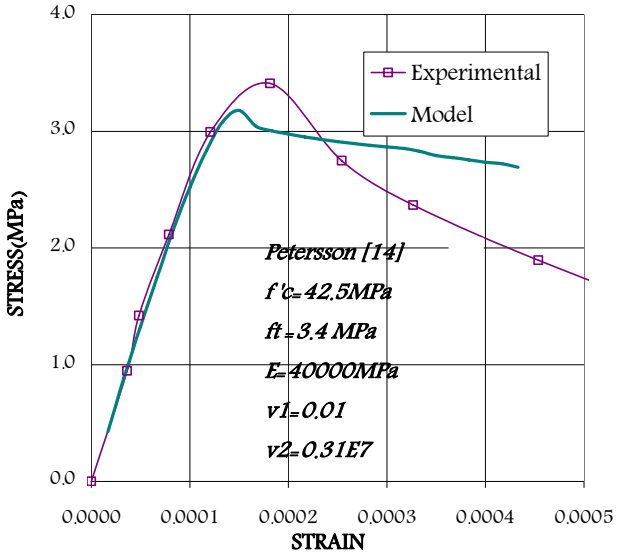

(a)

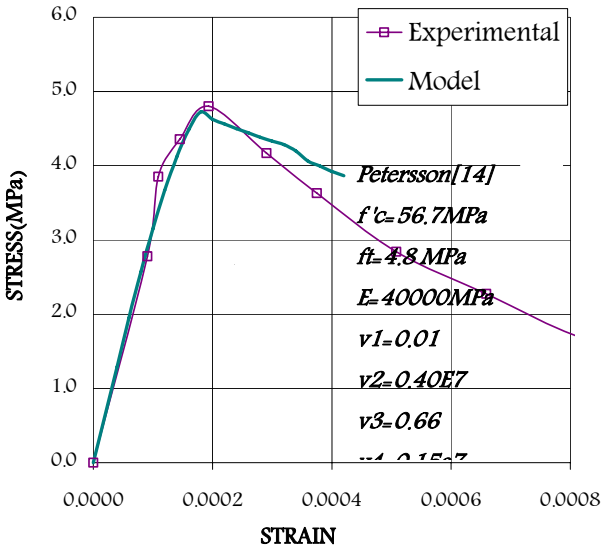

(b)

Figure 8. Comparison of model for uniaxial tension experimental data, petersson [14] (a) f'c = 42.5 (b) f'c = 56.7.

Figures 9 and 10 show the experimental data of Sfer [15] for triaxial test under low and high confinement with model results,They show that model predicts higher strength (7 %) in low confinement but it is close to experimental result.

5.2. Cyclic Loading Different states of cyclic loadings such as uniaxial compression, uniaxial compression, uniaxial compression-tension and proportional and non-proportional triaxial compression are considered for evaluation of model.

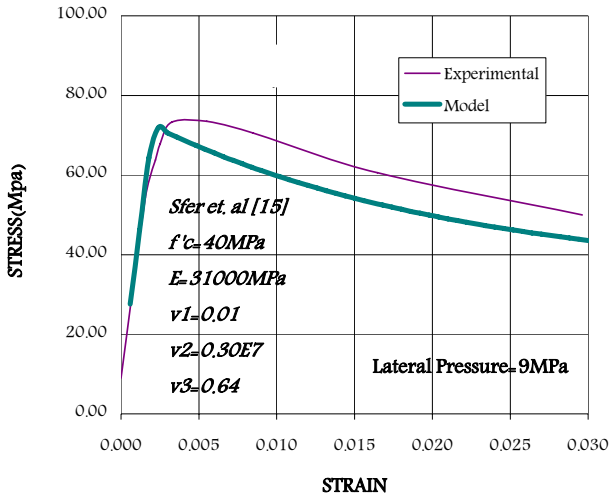

(a)

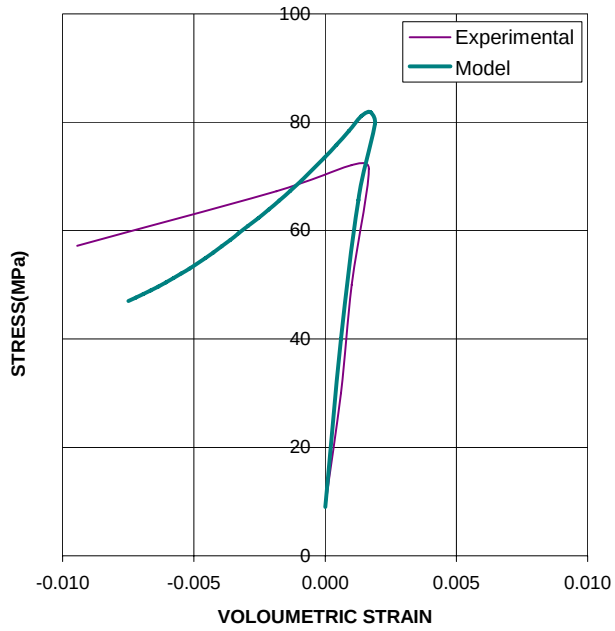

(b)

Figure 9. Comparison of model for triaxial compression experimental data (Low Confinement)-, Sfer [15] (a) Stress-strain curve (b) Volumetric strain versus stress.

Figure 11 shows the result of uniaxial compression cyclic loading of Sinha [16] with model prediction that shows close fitting between model result and experiment.

Figure 12 and 13 show the result of uniaxial cyclic tension and uniaxial tension alternate compression experimental test data of Reihardt [17] with model simulation that show a good result and fitness.

Figure 14 shows the result of cyclic shear test of Eligenhause [18] with model prediction that shows good prediction.

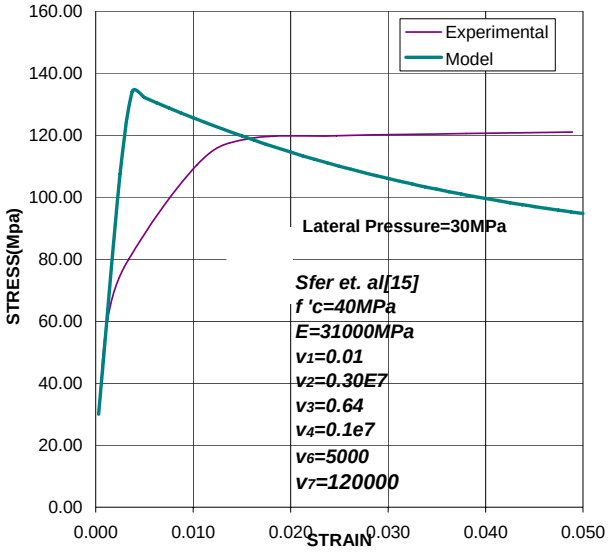

(a)

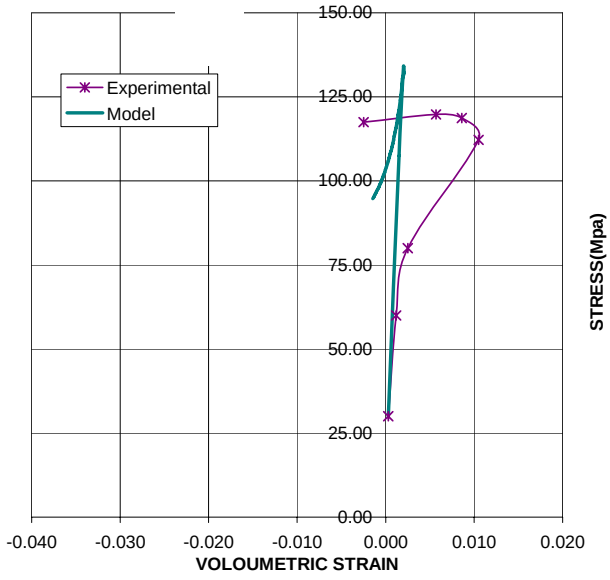

(b)

Figure 10. Comparison of model for triaxial compression experimental data (High Confinement)-, Sfer [15] (a) Stress-strain curve (b) Volumetric strain versus stress.

Figure 15 shows the result of hydrostatic compression of Bazant [19] with model prediction that shows very good fitting.

Figures 16 shows the comparison between Hurlbeut [20] test data for tri-axial compression with constant lateral pressure of 1Ksi (6.91 MPa) with model prediction and in Figure 17 the result of Scavuzzo, et al [21] triaxial compression test when the axial compression decreases with an increase in the lateral pressure, as cyclic loading is shown, that illustrate good fitting of model and experimental results.

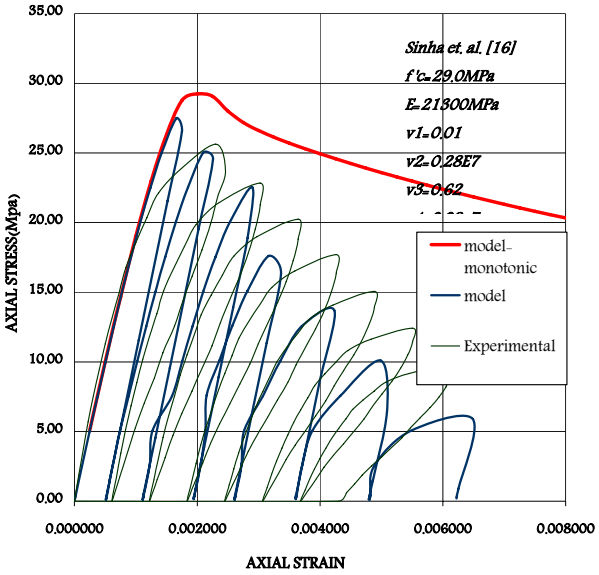

Figure 11. Comparison of model for cyclic uniaxial compression experimental data-Sinha, et al [16].

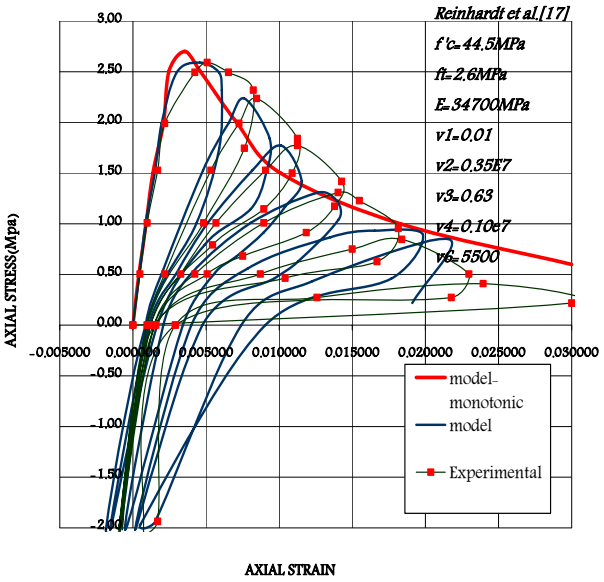

Figure 13. Comparison of model for cyclic compression-Tension experimental data-reinhardt [17].

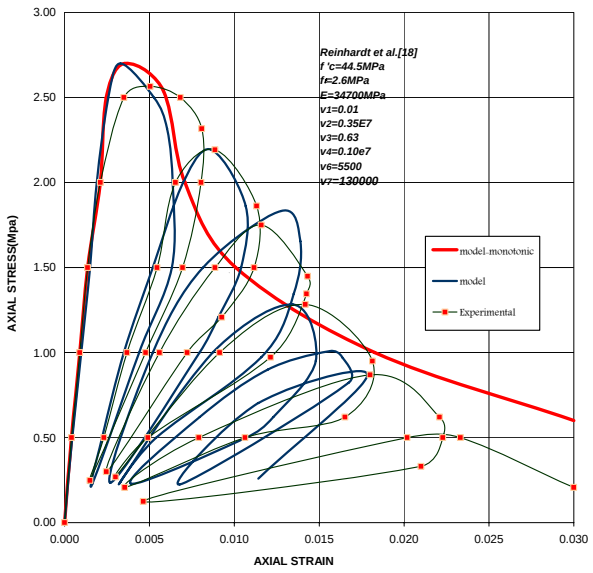

Figure 12. Comparison of model for cyclic tension experimental data-reinhardt [17].

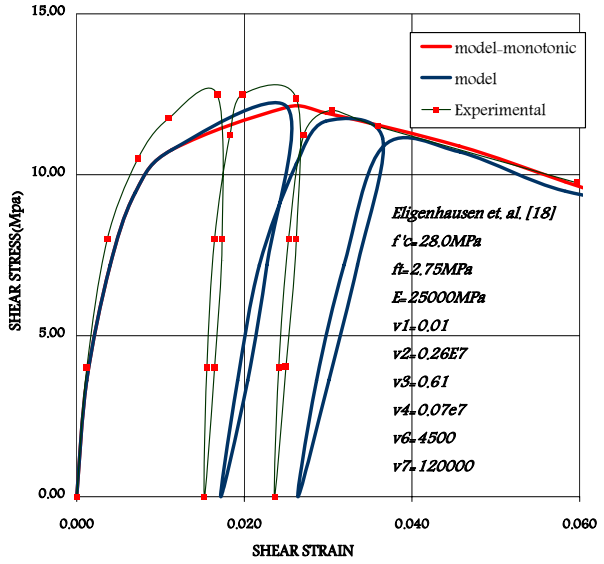

Figure 14. Comparison of model for cyclic shear stress experimental data-eligenhause [18].

6. CONCLUSIONS

From this research on the basis of substructure a model for simulation of concrete behavior under any stress/strain path in the multilaminate framework, with using sub-loading surface is derived. The comparison of model with experimental data such as monotonic uniaxial compression/tension, biaxial loading, triaxial compression and hydrostatic compression, show the good simulation of model. It

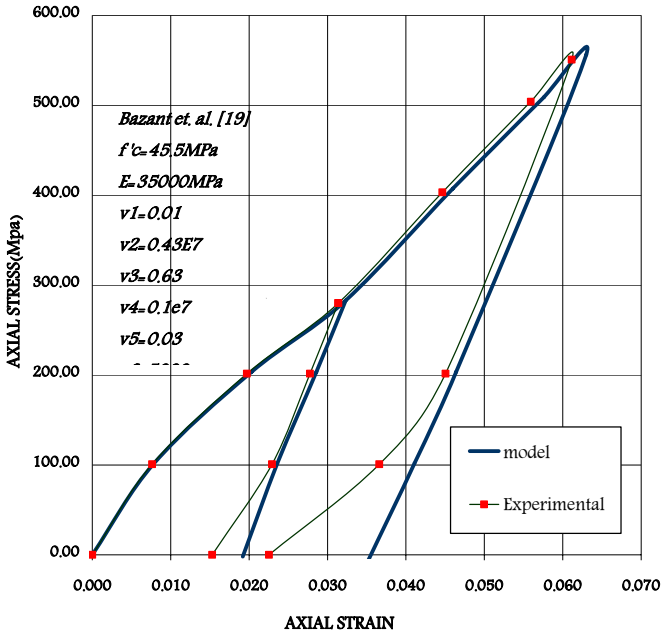

Figure 15. Comparison of model for cyclic Hydrostatic compression experimental data-Bazant, et al [19].

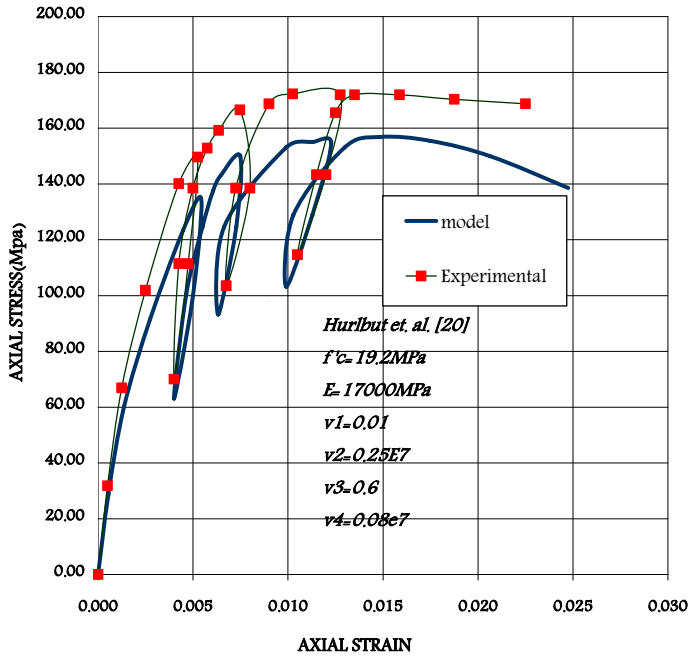

Figure 16. Comparison of model for cyclic tri-axial compression experimental data (Lateral pressure = 1 Ksi = 6.91 MPa) hurlbut, et al [20].

also shows the capability of the model to predict the behavior of concrete under any stress path such as uniaxial compression/tension hydrostatic, loading/reloading and cyclic triaxial compression.

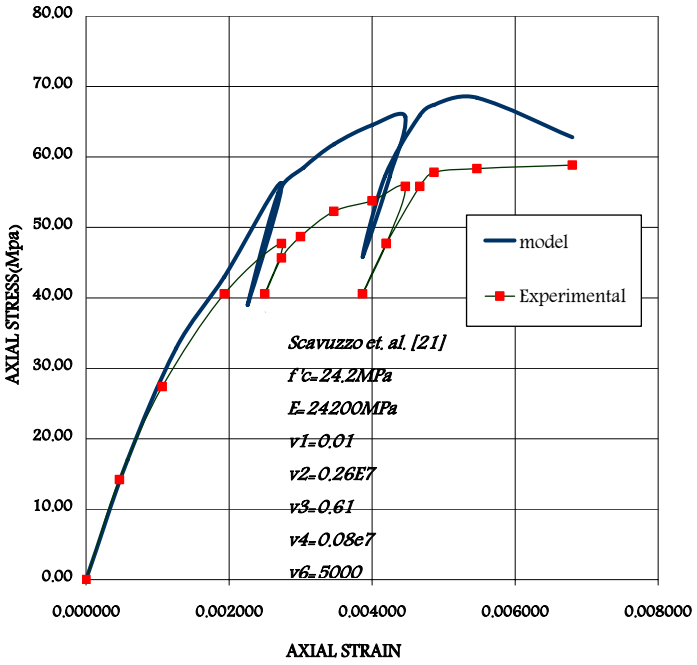

Figure 17. Comparison of model for cyclic tri-axial compression non-proportional experimental data-scavuzzo, et al [21].

7. REFERENCES

1. Taylor, G. I. "Plastic Strain in Metals", ***J. of Industrial Metals***, Vol. 62,(1938), 307-324.
2. Batdorf, S. B. and Budiansky, B., "A Mathematical Theory of Plasticity Based on the Concept of Slip", ***National Advisory Committee for Aeronautics***, TN 1871, (1949).
3. Zienkewics, O. C. and Pande, G. N., "Time Dependent Multi-Laminate Model of Rocks-A Numerical Study of Deformation of Rock Masses", ***Int. J. of Numerical and Analytical Methods in Geomechanics***, (1977), 219-247.
4. Pande, G.N. and Sharma, K. G., "Multilaminate Model of Clays-A Numerical Evaluation of the Influence of Rotation of Principal Stress Axes", ***Int. J. for Numerical and Analyt. Meth. in Geomech***, (1983), 397-418
5. Bazant, Z. P. and Oh, B. H., "Microplane Model for Fracture Analysis of Concrete Structures", ***Proceeding Symposium on the International of Non-Nuclar Munitions with Structures***, Us Air force Academy, (1983), 49-53.
6. Sadrnejad, S. A. and Pande, G. N., "A Multilaminate Model for Sands", ***Proceeding of 3rd International Symosium on Numerical Models in Geomechanics, NUMOG III***, Niagara Fall, Canada, (1989), 8-11.
7. Sadrnejad, S. A., "A Sub-Loading Surface Multilaminate Model for Elastic Plastic Porous Media", ***International Journal of Engineering***, Vol. 15, No.4, (2002), 315-324.
8. Hashiguchi, K., "Elastoplastic Constitutive Equations with Extended Low Rules", ***J. Fac. Agr***., Kyushu University, No. 38, (1994), 279-286.
9. Hashiguchi, K., "Guide-manual for Elastoplastic Constitutive Models Comparison of Elastoplastic Constitutive Models Emphasizing on Subloading Surface Model and Bounding Surface Model", http://www.Mech.Bpes.Kyushu-U.Ac.Jp/Index-E.Htm, Kyushu University website, (2005).
10. Bresler, B. and Pistler, K. S., "Strength of concrete under combined stresses", ***J. of Am.Conc. Inst***., Vol. 551, No. 9, (1958), 321-345.
11. Goode, C. D. and Helmy, M. A., "The Strength of Concrete Under Combined Shear and Direct Stress", ***Mag. of Conc. Research***, Vol. 19, No. 59, (1967), 179-200.
12. Tasuji, M. E., Slate, F. O. and Nilson, A. H., "Stress-Strain Response and Fracture of Concrete in Biaxial Loading", ***ACI J***., (July 1978), 306-312.
13. Van Mier, J. G., "Multiaxial Strain Softening of Concrete", ***J. of Mat. and Fracture***, Vol. 111, No. 19, 179-200.
14. Peterson, P. E., "Crack Growth and Development of Fracture Zone in Plain Concrete and Similar Materials", Rep. No. TVBM1006 Lund Institute of Technology, Sweden, (2001).
15. Sfer, D., Carol, I., Gettu, R. and Este, G., "Study of the Behavior of Concrete Under Triaxial Compression", ***ASCE-J. of Eng. Mech***., Vol. 128, No. 2, (2002), 156-

163.
16. Sinha, B. P.,Gerstel, K. H. and Tulin, L. G., "Stress-Strain Relations for Concrete Under Cyclic Loading", ***J. Am. Conc. Inst***, Vol. 62, No. 2, (1964), 195-210.
17. Reinhardt, H. W. and Cornelissen, H. A. W., "Post-Peak Cyclic Behaviour of Concrete in Uniaxial Tensile and Alternating Tensile and Compressive Loading", ***Cement and Concrete Research***, Vol. 14, (1984), 263-270.
18. Eligenhausen, R., Popov, E. P. and Bertero, V. V, "Local Bond Stress-Slip Relationships of Deformed Bars Under Generalized Excitations", Eartquake Engineering Research Center, College of Engineering, University of California, Bekeley, C.A. Report No. UCB/EERC-83/23, (1983).
19. Bazant, Z. P., Xiang, Y., Adley, M., Prat, P. C. and Akers, S., "Microplane Model for Concrete II, Data Delocalization and Verification", ***J. of Eng. Mech. ASCE***, Vol. 3, (1996), 263-268.
20. Hurlbert, B. J., "Experimental and Computational Investigation of Strain Softening in Concrete", Report AFOSR 80-0273, US Air Force Office of Scientific Research, University of Colorado, Boulder, U.S.A., (1985).
21. Scavuzzo, R., Stancowski, T., Gerstle, K. and Ko, H. Y., "Stress-Strain Curves for Concrete Under Multiaxial Load Histories", NSF CME 80-01508 Dep. Of CEAE, University of Colorado, Boulder, U.S.A., (1983).